

Development and Validation of Corridor Flow Submodel for CFAST

J. L. BAILEY,^{1*} G. P. FORNEY,² P. A. TATEM¹ AND W. W. JONES²

¹*Naval Research Laboratory, 4555 Overlook Ave. SW,
Washington, D.C. 20375 USA*

²*National Institute of Standards and Technology, 100 Bureau Dr.,
MS 8663, Gaithersburg, MD, 20899 USA*

ABSTRACT: The modeling of fire and smoke spread is an evolving field. As knowledge is acquired and resources become available, models are enhanced to make their predictions more accurate and/or their computations faster. This paper will discuss the Consolidated Fire and Smoke Transport (CFAST) zone fire model, developed by the National Institute of Standards and Technology (NIST), and a recent addition to that model, referred to as the Corridor Flow Submodel. The goal of this new submodel is to more accurately predict the flow of smoke down a corridor which has an impact on fire protection issues such as detection and escape time. Prior to the addition of this new submodel, CFAST assumed that smoke traveled instantly from one side of a compartment to another. Development of the submodel will be discussed and then the enhanced CFAST, Version 4.0.1 (executable dated 3/8/00), will be used to model a real-scale experiment conducted onboard the ex-USS SHADWELL, the Navy's R&D Damage Control platform.

KEY WORDS: fire modeling, smoke movement, full-scale experiment, model validation.

INTRODUCTION

CFAST [1] USES the standard zone model assumption that the atmosphere inside a compartment is generally divided into an upper and lower layer. Each layer is assumed to be of uniform temperature and composition. Consequently, the moment hot gases enter a compartment, CFAST calculates a hot gas layer which covers the entire ceiling. All areas under the ceiling have the same temperature. If hot gases were entering a corridor from one end, CFAST would predict that the temperature at the far end

*Author to whom correspondence should be addressed. E-mail: jbailey@custor.nrl.navy.mil

would immediately increase. The assumption is made that the temperature change takes place instantaneously, so the transient time to fill the area is ignored. In reality, there is a delay as the **hot** gases travel down the corridor.

This paper proposes a simple procedure for accounting for the formation delay of an upper layer in a long corridor by using correlations developed from numerical experiments generated with the three-dimensional Large Eddy Simulation (LES3D) field model [2]. Two parameters related to corridor flow are then estimated, the time t_c required for a ceiling jet to travel in a corridor and the temperature distribution down the corridor.

As soon as the ceiling jet reaches the end of the corridor, CFAST reverts back to the two-layer assumption, i.e., the model uses the amount of energy and mass in the upper layer to calculate an average temperature. By definition, the atmosphere at all locations within the upper layer is at this average temperature. In other words, the new submodel allows for a more detailed depiction of the temperature distribution at the ceiling level only as the ceiling jet is traveling the length of the corridor.

Although the new submodel contains features which are not restricted to the corridor compartment [3], they will not be explored in this validation. These additional **features**, which relate to how the ceiling jet affects compartments adjacent to the corridor compartment, will not be discussed. This validation focuses on the ceiling jet flow within the corridor compartment and compares experimental results and model predictions for the corridor compartment only.

THEORY

This section outlines the procedure used for estimating a ceiling jet's temperature decay, depth, velocity and, hence, arrival time at each point in a corridor. A field model, LES3D [2], is used to model corridor flow for a range of inlet ceiling jet temperatures and depths. Inlet velocities are derived from the inlet temperatures and depths. For each model run, the average ceiling jet temperature and velocity are calculated as a function of distance down the corridor. The temperature and velocity **down** the corridor are then correlated. CFAST uses these correlations to estimate conditions in the corridor.

Assumptions

The assumptions made in order to develop the correlations are:

- The time scale of interest is the time required for a ceiling jet to traverse the length of the corridor. For example, for a 100 m corridor with 1 m/s flow, the characteristic time period would be 100 s.

- Cooling of the ceiling jet due to mixing with adjacent cool air is large compared to cooling due to heat loss to walls. In addition, we assume that walls are adiabatic. This assumption is conservative. An adiabatic corridor model predicts more severe conditions downstream in a corridor than a model that accounts for heat transfer to walls, since cooler ceiling jets travel slower and not as far.
- We do not account for the fact that ceiling jets that are sufficiently cooled will stagnate. Similar to the previous assumption, this assumption is conservative and results in over predictions of conditions in compartments connected to corridors (since the model predicts that a ceiling jet may arrive at a compartment when in fact it may have stagnated before reaching it).
- Ceiling jet flow is buoyancy driven and behaves like a gravity current. The inlet velocity of the ceiling jet is related to its temperature and depth.
- Ceiling jet flow lost to compartments adjacent to the corridor is not considered when estimating ceiling jet temperatures and depths. Similarly, a ceiling jet in a corridor is assumed to have only one source.
- The temperature and velocity at the corridor inlet are constant in time.
- The corridor height and width do not affect a ceiling jet's characteristics. Two ceiling jets with the same inlet temperature, depth and velocity behave the same when flowing in corridors with different widths or heights as long as the inlet widths are the same fraction of the corridor width.
- Flow enters the corridor at or near the ceiling. The inlet ceiling jet velocity is reduced from the vent inlet velocity by a factor of $w_{\text{vent}}/w_{\text{room}}$ where w_{vent} and w_{room} are the widths of the vent and room, respectively.

Ceiling Jet Characteristics

Compartments with Length to Height Ratios Near One - Normal Rooms

In a normal compartment where the length to height ratio is near one, ceiling jet velocities can be estimated from correlations [4,5], or by solving the horizontal momentum equation in addition to the mass and energy conservation equations.

Smoke flow in a normal room is qualitatively different from smoke flow in a corridor in one important respect. Corridor smoke spreads mainly in one dimension, along the length of the corridor. Smoke spreads in a normal room, on the other hand, in two dimensions. In addition, assuming no friction or heat transfer to boundaries, ceiling jet velocities in corridors will be essentially constant while ceiling jet velocities in normal rooms will be

approximately proportional to $1/r$ (where r = distance from the centerline of the plume). This arises since the surface area at the exterior boundary is proportional to r , then the velocity must be proportional to $1/r$ so that the mass flow out remains equal to the mass flow in. As a result, these correlations are not valid for estimating ceiling jet velocities in corridors.

If the length to height ratio of the room of fire origin is near one, then ceiling jet traversal times may be estimated using the velocity correlation for a steady state fire.

$$u(r) = \begin{cases} 0.96 \left(\frac{Q}{H} \right)^{1/3}, & (r/H) \leq 0.15 \\ 0.195 \frac{(Q/H)^{1/3}}{(r/H)^{5/6}}, & (r/H) > 0.15 \end{cases} \quad (1)$$

found in Kefrence [4] where H is the ceiling height (m), Q is the total energy release rate of the fire (kW), r is the distance from the plume centerline (m) and u is the velocity (m/s). CFAST [1] estimates ceiling jet temperatures and velocities using a correlation derived by Cooper, given in Reference [5].

The time, $t(r)$, required for the jet to travel a distance r from the source can then be obtained from the velocity by integrating the quantity $dr/u(r)$. Using the correlation given in Reference [4] we obtain

$$\left| \frac{r}{6.4q} + \frac{r^2}{11.6q} \right|$$

where, $s = r/(0.15H)$ and $q = (Q/H)^{1/3}/H$. The time $t(r)$ corresponding to Cooper's velocity correlation must be integrated numerically. There is no analytic formula for $t(r)$ since the calculation depends on a correlation that is obtained numerically. The arrival time is approximately proportional to r^2 , the distance squared, for $s > 1$. It will be shown later empirically that in a corridor the arrival time is proportional to the distance, r .

Compartments with Large Length to Height Ratios **Corridors**

The correlations defined by Equations (1) and (2) are not appropriate in corridors. Ceiling jet flow in a corridor can be characterized as a one-dimensional gravity current. To a first approximation, the velocity of the current depends on the difference in density between the gas located at the leading edge of the current and the gas in the adjacent ambient air.

The velocity also depends on the depth of the current below the ceiling. A simple formula for the gravity current velocity may be derived by equating the potential energy of the current, $mgd_0/2$, measured at the half-height $d_0/2$ with its kinetic energy, $mU^2/2$, to obtain

$$U = \sqrt{gd_0} \quad (3)$$

where m is mass, g is the acceleration of gravity, d_0 is the thickness of the gravity current and U is the velocity. When the density difference, $\Delta\rho = \rho_{\text{amb}} - \rho_{\text{cj}}$, between the current and the ambient fluid is small, the velocity U is proportional to

$$\sqrt{gd_0 \frac{\Delta\rho}{\rho_{\text{cj}}}} \rightarrow \sqrt{gd_0 \frac{\Delta T}{T_{\text{amb}}}} \quad (4)$$

where ρ_{amb} , T_{amb} are the ambient density and temperature, ρ_{cj} , T_{cj} are the density and temperature of the ceiling jet, and $\Delta T = T_{\text{cj}} - T_{\text{amb}}$ is the temperature difference. Here, use has been made of the ideal gas law, $\rho_{\text{amb}}T_{\text{amb}} \approx \rho_{\text{cj}}T_{\text{cj}}$.

This can be shown by using an integrated form of Bernoulli's law, noting that the pressure drop at the bottom of the ceiling jet is $\Delta P_b = 0$, the pressure drop at the top is $\Delta P_t = gd_0(\rho_{\text{cj}} - \rho_{\text{amb}})$ and using a vent coefficient $C_{\text{vent}} = 0.74$, to obtain

$$U \approx 0.7 \sqrt{gd_0 \frac{\Delta T}{T_{\text{amb}}}}$$

Formulas of the form of Equation (5) lead one to conclude that the characteristics of a ceiling jet in a corridor depend on its depth, d_0 , and relative temperature difference, $\Delta T/T_{\text{amb}}$. Therefore, as the jet cools, it slows down, due to the factor $\Delta T/T_{\text{amb}}$. If no heat transfer occurs between the ceiling jet and the surrounding walls, then the **only** mechanism for cooling is mixing with surrounding cool air.

Numerical Experiments

Qualitative Numerical Corridor Flow Experiments

Figures 1-4 are presented to illustrate how various boundary conditions (adiabatic walls, cold walls, etc.) affect qualitative ceiling jet characteristics. These simulations were performed using LES3D. As can be seen from Figures 1 and 2, a ceiling jet modeled in an enclosure with adiabatic walls travels

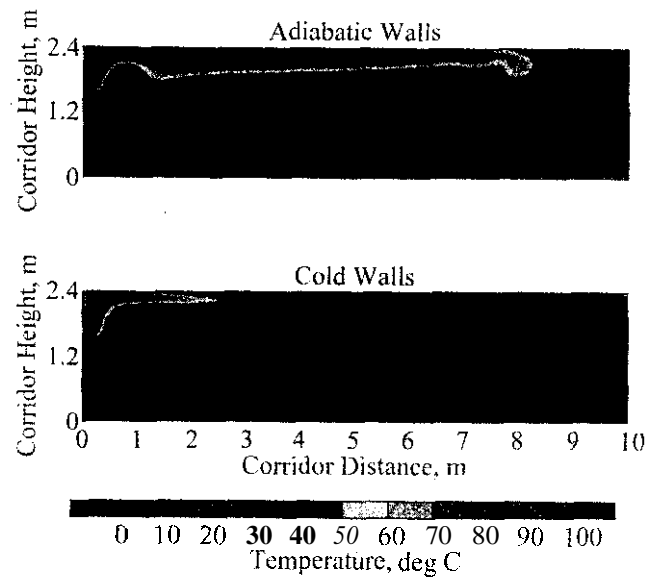


Figure 1. Shaded temperature contours along the corridor centerline for two temperature boundary conditions. The inlet flow has a depth of 0.6 m, a velocity of 1.0 m/s and a temperature rise of 300°C above ambient. A no-slip boundary condition is imposed at all wall surfaces.

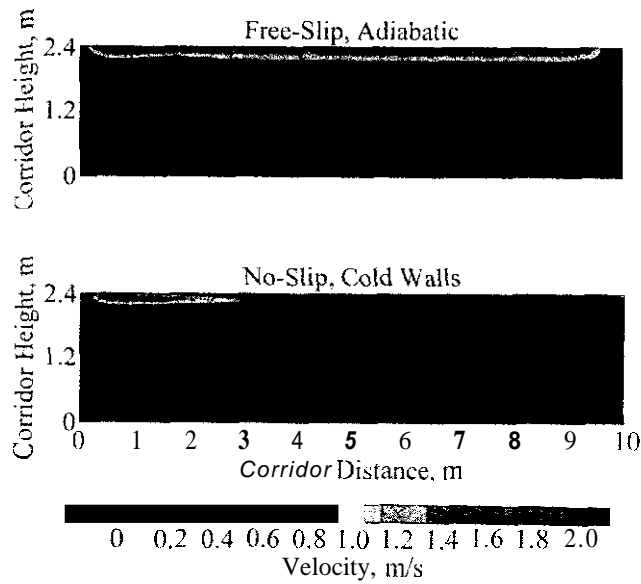


Figure 2. Shaded velocity contours along the corridor centerline for two different boundary conditions. The inlet flow has a depth of 0.6 m, a velocity of 1.0 m/s and a temperature rise of 300°C above ambient.

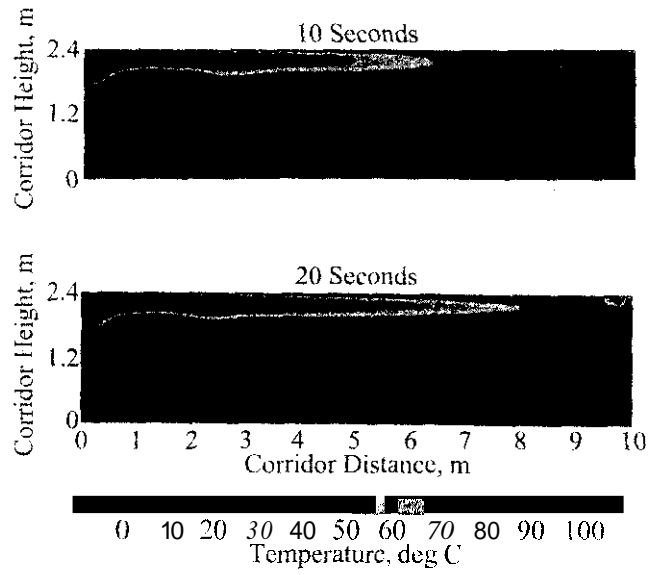


Figure 3. Shaded temperature contours along the corridor centerline at two different times during the simulation. The inlet flow has a depth of 0.6 m, a velocity of 1.0 m/s and a temperature rise of 300°C above ambient.

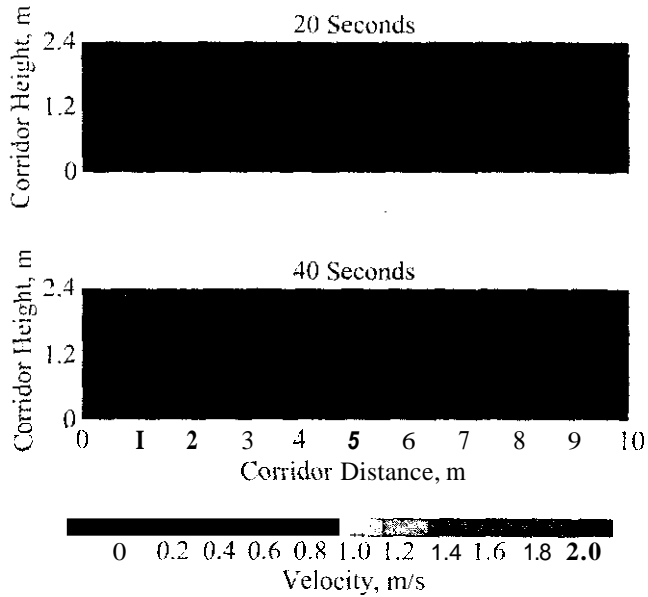


Figure 4. Shaded velocity contours along the corridor centerline at two different times during the simulation. The inlet flow has a depth of 0.6 m, a velocity of 1.0 m/s and a temperature rise of 312 C above ambient.

farther and faster than a ceiling jet modeled with cold walls. Figure 3 shows shaded temperature contours in a vertical plane along the centerline of a 10 m corridor at 10 and 20 s. The temperature distribution at these two times is about the same. Even though an individual portion of smoke has moved up to 10 m, the peak temperature (edge of darkest contour) has only shifted by about 1 m, from 5 to 4 m. Similarly, Figure 4 shows shaded velocity contours in a vertical plane along the centerline of a 10 m corridor at 20 and 40 s. The velocity distribution does not change appreciably between the two times. Because of this, we assume that the walls do not heat up and that the temperature and velocity distributions quickly reach steady state.

The Parameter Study

In order to better understand the effects of the inlet ceiling jet temperature and depth on its characteristics downstream in a corridor, a number of numerical experiments were performed using the field model LES3D. Twenty cases were run with five different inlet depths and four different inlet temperatures.

The inlet ceiling jet depths, d_0 , used in the parameter study are 0.15, 0.30, 0.45, 0.60 and 0.75 m. The inlet ceiling jet temperature rises, ΔT_0 , used in the parameter study are 100, 200, 300 and 400 °C. Velocities using Equation (5) corresponding to these inlet depths and **temperature** increases are given in Table 1.

For each case, a nonslip velocity boundary condition was imposed at all solid boundaries. Adiabatic thermal boundary conditions were imposed at the walls to simulate no heat transfer to wall surfaces. A vertical symmetry plane along the centerline of the corridor was used to reduce the number of grids, thereby improving the resolution. An open boundary condition was imposed at the far end of the corridor.

The simulated corridor had dimensions of 10 m \times 2.4 m \times 2.4 m. Each grid cell had dimensions of approximately 10 cm \times 5 cm \times 2.5 cm, where the

Table 1. Inlet velocity (m/s) as a function of inlet temperature and depth.

Depth (m)	Temperature Excess (°C)			
	+ 100	+ 200	+ 300	+ 400
0.15	0.50	0.71	0.87	1.00
0.30	0.71	1.10	1.22	1.41
0.45	0.87	1.22	1.50	1.73
0.60	1.00	1.41	1.73	2.00
0.75	1.12	1.58	1.94	2.24

longest grid dimension occurred along the length of the corridor. Approximately 220,000 grid cells were used to model the corridor, 24 across the width of the corridor and 96 along both the height and length of the corridor. For most cases, a Reynolds number of 9,200 (approximately 96^2) was used to resolve the small-scale flow features. A coarser grid with dimensions 10 cm x 5 cm x 5 cm was used initially. It was found that the vertical grid dimension of 5 cm was not sufficiently small to resolve the thin, 0.15 m ceiling jet cases.

The computational fluid dynamic or field model, LES3D, calculates temperatures, pressures and velocities at many points in the three-dimensional rectangular grid. These data are reduced to a more manageable size by noting that the inlet high-temperature ceiling jet flow stratifies the corridor gases into two regions, an upper region of hot, fast flowing air and a lower region of relatively cool quiescent air. For each vertical plane along the length of a corridor, a layer interface height is estimated by using the distance above the floor where the temperature gradient is greatest. An upper layer temperature $T_U(i)$ is calculated by averaging all temperatures in the slice above the estimated layer height.

Summary of Results

Ceiling Jet Temperatures

The upper layer temperature rise above ambient for each slice is given by $\Delta T(i) = T_U(i) - T_{amb}$. These temperature rises are scaled by the inlet temperature rise, ΔT_0 , and transformed using $\log(\Delta T/\Delta T_0)$. The resulting data are presented in Figure 5. Note that each plot is nearly linear and that all plots (except for the $d_0 = 0.15$ m group) lie within a single group. This implies that the relative temperature falloff is independent of the inlet temperature rise and depth (assuming that the inlet depth is sufficiently thick). The temperature curves presented in Figure 5 were approximated by straight lines using a linear least squares curve fitting procedure. This fit is given in the form of

$$\log\left(\frac{\Delta T}{\Delta T_0}\right) = a + bx. \quad (6)$$

This is equivalent to

$$\frac{\Delta T}{\Delta T_0} = C_1 10^{bx} \rightarrow C_1 \left(\frac{1}{2}\right)^{x/h_{0.2}} \quad (7)$$

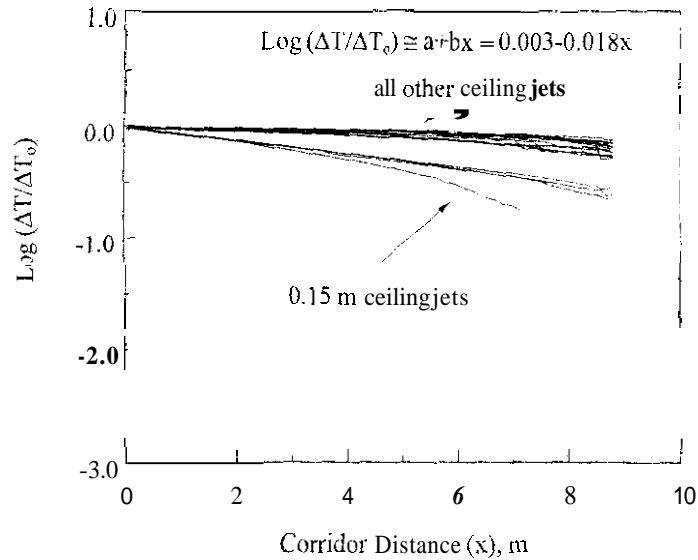


Figure 5. Log., of the relative temperature excess downstream in a corridor using an adiabatic temperature boundary condition for several inlet depths and inlet temperature rises

where $C_1 = 10^a$ and $h_{1/2} = -\log(2)/b$. The parameter $h_{1/2}$ in Equation (7) has a physical interpretation. It is the distance down the corridor where the temperature rise, ΔT , falls off to 50% of its original value or equivalently, $\Delta T(h_{1/2}) = 0.5 \Delta T_0$.

The half-distance, $h_{1/2}$, can be approximated by $h_{1/2} = \log(2)/0.018 \approx 16.7$, where $b = -0.018$ is given in Figure 5. Similarly, the coefficient C_1 is approximated by $C_1 = 10^a = 10^{0.003} \approx 1$ where a is also given in Figure 5. Therefore, the temperature rise, ΔT , may be approximated by

$$\Delta T = \Delta T_0 \left\{ \frac{x}{h_{1/2}} \right\}^{-2}$$

Ceiling Jet Arrival Times

Numerical thermocouples were placed 0.15 m below the ceiling every 0.5 m along the centerline of the corridor for all cases except for the $d_0 = 0.15$ m cases, where they were placed 0.075 m below the ceiling. Ceiling jet arrival times were recorded by noting when the temperatures rose 1°C. The arrival time for each case was scaled by the ceiling jet velocity, U_0 , at the entry vent. These reduced data are displayed in Figure 6. Note that most arrival time curves lie within approximately the same region. A group of curves, corresponding to the inlet depth of $d_0 = 0.15$ m, are separate from the

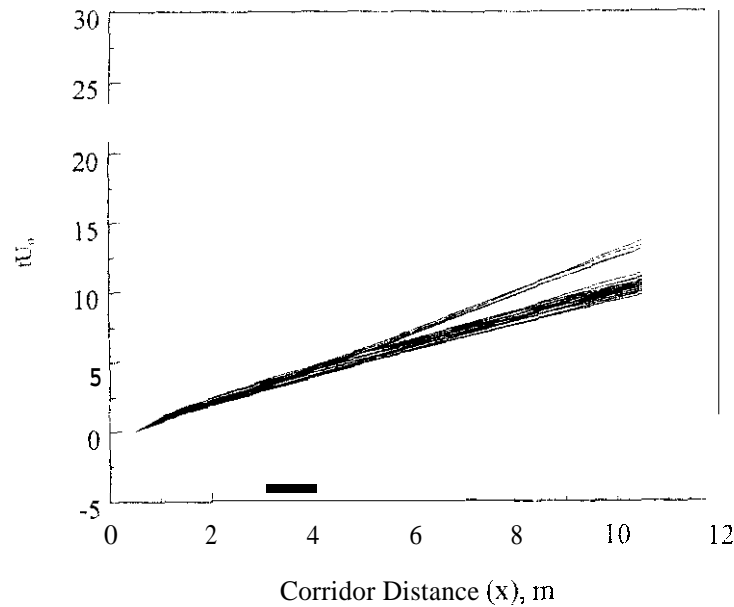


Figure 6. Ceiling jet arrival time as a function of distance down the corridor scaled by the initial ceiling jet velocity, U_0 , for several initial inlet depths and temperature rises. The walls are adiabatic. The inlet velocity, U_0 , is given by Equation (5). The arrival time of the ceiling jet is measured by noting when its temperature rises 1°C above ambient at a given distance downstream from the inlet.

main group. This is because the 0.15 m ceiling jets are weaker than the remainder. They lose their driving potential, resulting in lower velocities and hence greater arrival times. The arrival time of the ceiling jet head may be approximated by $t = x/U_0$ for all d_0 except for $d_0 = 0.15$ in.

EXPERIMENT SELECTION

The experiment that was selected to validate the new submodel was part of the 688/SHADWELL test series [6]. The objective of this test series was to develop, test, and validate improved ventilation doctrine for submarine fires. These experiments were not designed to provide data for a model validation. Consequently, the experimental data were inspected, prior to beginning the model validation, to verify that sufficient data **existed** to provide a meaningful comparison with model predictions. Knowledge of the experimental results was never used to adjust the model input unless explicitly stated in this validation report.

A section of the port wing wall on ex-USS SHADWELL [7] was configured to represent the forward compartment of an SSN 688 Class

submarine. The test area was comprised of 14 compartments, located on four levels. The compartments were connected with various hatches, watertight doors, and a mechanical ventilation system. The experiments consisted essentially of igniting a pan fire in one of the compartments and then manipulating variables to observe the effect on the smoke flow within the test area.

There was only one compartment within the test area, the Laundry Room, which contained a corridor. Both exhaust and supply terminals were located near the ceiling in the corridor of this compartment. The Corridor Flow Submodel does *not* take into account any effects of forced ventilation on the **flow** of the ceiling jet. Therefore, an experiment which employed the mechanical ventilation system would not be suitable for comparison to model predictions. Standard experimental procedure called for utilizing the mechanical ventilation system for at least the first minute after ignition of the pan fire. There was one experiment **in** which the mechanical ventilation system was secured and the supply **and** exhaust terminals *were* blocked **off**. This experiment, denoted as sub4-10, occurred on January 29, 1996, and was used for validation purposes.

CONFIGURATION

The Laundry Room was located on the third level, between Frame 81 and Frame 88. The port side was bounded by the hull and the Well Deck bounded the starboard side. The compartment **was** actually divided into two subcompartments (Figure 7). The subcompartment which contained the fire will be referred *to* as the Fire Compartment and the remaining subcompartment will be referred to as the Passageway. The Laundry Room was 8.51 m long, 2.57 m high, and varied in width from 3.86 m on one end (at Frame 88) *to* 4.11 m on the other (at Frame 81). The Fire Compartment was 6.10 m long and 1.75 m wide. The Passageway consisted of the remainder of the Laundry Room. Its dimensions will be discussed later under the section entitled "Model Input."

There was a door, 0.66 m wide and 1.93 m high, which connected the Fire Room to the Passageway. This door did not have a sill, **but** it did have a 0.67 m soffit. There were two open watertight doors, one in the bulkhead at Frame 81 and one in the bulkhead at Frame 88 connecting the Passageway to the compartments on either side. These doors were 0.66 m wide and 1.68 m high, with 0.23 m sills and 0.68 m soffits. There was also a hatch, 0.91 m x 0.76 m, in the Passageway overhead to the compartment above. Stringers ran athwartship at 1.22 m intervals from Frame 81 to Frame 88. These protruded **from** the overhead by approximately 22 cm.

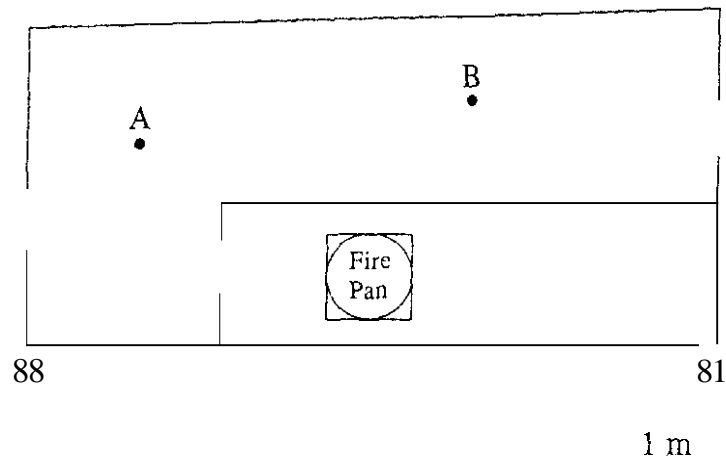


Figure 7. Plan View of Laundry Room drawn to scale; subdivided into Fire Compartment and Passageway

The partition which divided the Laundry Room was 0.318 cm thick steel. Referring to Figure 7, the in-board Laundry Room bulkhead, between Frame 81 and Frame 88, which comprised one side of the Fire Compartment, was 1.27 cm thick steel. The opposite bulkhead was 1.59 cm thick steel, up 1.8 m from the deck. The rest of the bulkhead, up to the overhead, was 1.91 cm thick steel. The bulkheads at Frame X1 and Frame XX, as well as the deck and overhead, were all constructed of steel 0.95 cm thick.

The Fire Compartment contained a 1.05 m diameter fuel pan, 0.19 m above the deck. The pan was filled to approximately 9 cm with diesel fuel. Immediately prior to ignition, an unknown, but relatively small, amount of heptane was added to facilitate ignition of the diesel fuel.

INSTRUMENTATION

The discussion here will be limited to the instrumentation that was used for validation purposes.

The Fire Compartment contained a thermocouple string with six thermocouples. These were located nominally at 2.5, 2.0, 1.5, 1.0, 0.5 and 0.05 m above the deck. The string was 1.75 m aft of Frame 81 and 1.28 m port of the Well Deck bulkhead. The Passageway contained a similar thermocouple string positioned at Location 4 in Figure 7. The hatch in the Passageway overhead, mentioned above, was instrumented with a bi-flow probe and thermocouple. The position is denoted as Location B in Figure 7. The thermocouples were Type K, inconel-sheathed. The gas inside

the Fire Compartment was sampled at a point approximately 2.49 m above the deck, 4.90 m aft of Frame 81 and 1.27 m port of the Well Deck bulkhead. The computer system onboard ex-USS SHADWCLL collects and records data from the instruments once per second.

MODEL INPUT

The accuracy of a model's predictions is, of course, heavily dependent upon the accuracy of the information given as input. There are two instances where accuracy must be compromised. One instance occurs when the information is simply not known. An estimate must then be made in order for a prediction to result. The other occurs when the model cannot handle the actual configuration of the experiment. Again, an estimate must be provided to the model. This section will discuss the estimates used as input to CFAST for the validation of the Corridor Flow Submodel.

The mass loss rate is one of the key input parameters that the user must provide to CFAST. Although a load cell was used to measure the mass loss of fuel with time as the diesel burned, the normal variability of the load cell data was large compared to the amount of fuel burned during the time of interest. Therefore, the information from this device could not be used to calculate a mass loss rate. This input had to be estimated based on the temperature data from inside the Fire Compartment. CFAST predicts an upper and lower layer temperature for each compartment. Different mass loss rate estimates were used as input until the upper layer temperature in the Fire Compartment, as predicted by CFAST, matched the upper layer temperature calculated from experimental data.

There are various methods to translate the experimental temperature readings, measured at distinct locations, to the overall zone temperature. Sometimes the experimental data show a relatively large difference between two adjacent thermocouple readings which denotes a layer interface. In this experiment, as time progressed, the readings from the top four thermocouples deviated from the bottom two thermocouples. The average of the top four thermocouple readings was interpreted to reflect the upper layer temperature, and the average of the bottom two thermocouple readings was interpreted to reflect the lower layer temperature. An alternate method involves assigning the thermocouples to either the upper or lower layer depending on their relation to the interface height predicted by CFAST. At each second, the thermocouples located above the model-predicted interface height were averaged and used to represent the experimental upper layer temperature. Both methods resulted in essentially the same experimental upper layer temperature. An estimate for the mass loss rate was made by using different mass loss rate estimates as input until the upper layer

temperature in the Fire Compartment, as predicted by CFAST, matched this experimental upper layer temperature.

CFAST can only model compartments which are rectangular parallelepipeds. As mentioned previously, the Laundry Room contained a partition which divided it into two subcompartments. The Fire Compartment was a rectangular parallelepiped, but the Passageway was an L-shaped compartment. The Passageway had to be approximated as an equivalent rectangular parallelepiped so its dimensions could be interpreted by CFAST. For the purposes of the following discussion, the Passageway was divided into four sections shown in Figure 8. The separation between Sections 1 and 2 was defined by the midpoint of the door to the Fire Compartment. All four sections had the same height as the Laundry Room, 2.57 m. The remaining dimensions of the four sections are as follows: Section 1 - 0.95 m x 2.39 m, Section 2 - 0.80 m x 2.39 m, Section 3 - 2.11 m x 2.39 m, Section 4 - 6.10 m x 2.24 m. These dimensions are the measurements of the compartment at the overhead level. One wall of Sections 3 and 4, which corresponds to the hull of the ship, tapers out slightly. The dimensions stated above were the average width of these two sections.

When the DETECT keyword is utilized along with the Corridor Flow Submodel, the configuration must be modified so that the ceiling jet starts at one end of the compartment serving as the corridor. Therefore, the Passageway had to be redefined as consisting of Sections 2-4. The ceiling jet entered the Passageway as it flowed under the soffit of the Fire Compartment door. The ceiling jet then continued down the Passageway toward Location A and around the corner, passing Location B, until it

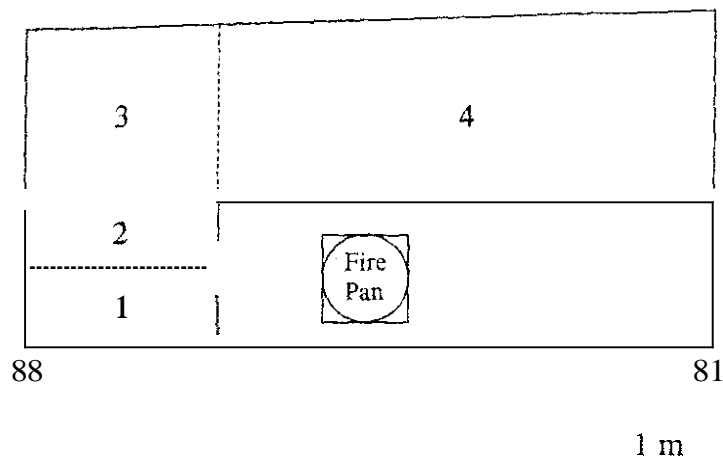


Figure 8. Plan view of Laundry Room, drawn to scale: Passageway divided into four sections.

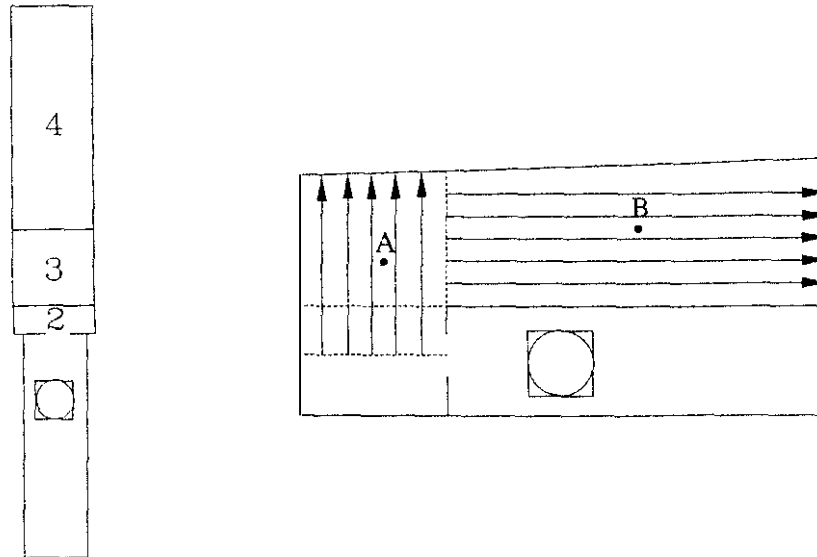


Figure 9. Initial Laundry Room configuration approximated for model input and resulting path of ceiling jet flow

reached the **end** of the Passageway. Initially, the most reasonable method of transforming the L-shaped Passageway into a rectangular parallelepiped appeared to be to simply “straighten” it out. i.e., align Sections 2-4. The length would be the sum total of Sections 2-4: $0.80\text{ m} + 2.11\text{ m} + 6.10\text{ m} = 9.01\text{ m}$. Using this approximation, the ceiling jet would flow all the way through Section 3 before it started toward Location B as shown by the arrows in Figure 9. This appears to be appropriate for modeling the flow to Location A, *but* not to Location B.

An alternate approximation was devised. The dividing line between Sections 3 and 4 was aligned with the dividing line between Sections 2 and 3 (Figure 10). Section 3 is now imbedded within Section 4. The ceiling jet heads toward Location A at the same time it flows around the corner and heads toward Location B. This appears to be a more realistic approximation and was used for the model validation. The final dimensions used as model input were: height = 2.57 m, length = $0.80\text{ m} + 6.10\text{ m} = 6.90\text{ m}$, width = 2.26 m. Note, the width was calculated using the actual overhead surface areas and the lengths of Sections 2 and 4.

A comment on the use of the Corridor, Flow Submodel is in order at this point. In general, the actual compartment dimensions should be used for model input. In this case, the Passageway dimensions had to be modified to accommodate the limitations of the submodel (ceiling jet entering at a point other than the end of the corridor and the presence of

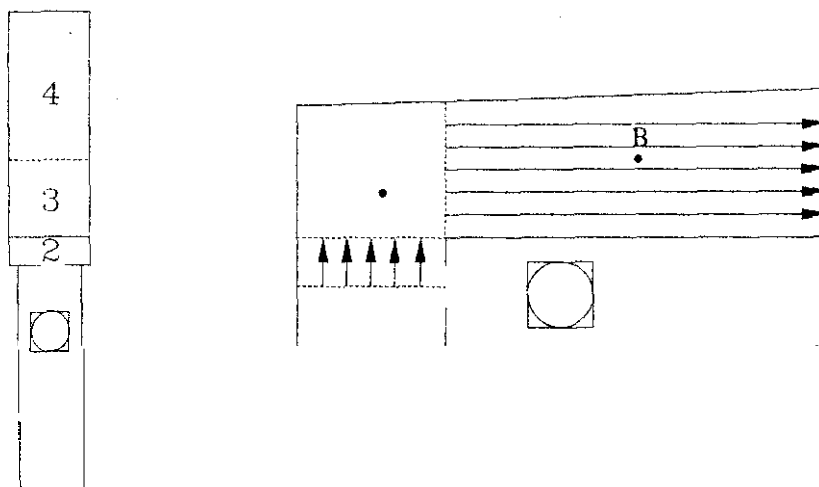


Figure 10. Alternate Laundry Room configuration approximated for model input and resulting pall; of ceiling jet flow

a corner). Since the Corridor Flow Submodel is only in effect while the ceiling jet is traveling down the corridor, these adjusted dimensions are no longer needed once the ceiling jet reaches the end of the Passageway. However, even if the actual dimensions were substituted at this point, subsequent model predictions would still be affected by the prior use of the adjusted dimensions. Therefore, model predictions were generated, from time zero, using both the actual and adjusted compartment dimensions. The predictions resulting from the use of the adjusted dimensions were used while the ceiling jet was traveling down the Passageway. For the times after the ceiling jet reached the end of the Passageway, the model predictions resulting from the use of the actual dimensions from time zero were used.

CFAST models the six surfaces of a rectangular parallelepiped as three separate entities: a ceiling, a floor, and the four walls. Each entity is allowed to consist of a distinct material with a distinct thickness. However, the entire ceiling is assumed to be homogenous, as are the other two entities. Note, that in this experiment, this assumption holds for decks (floors) and overheads (ceilings) in both the Fire Compartment and Passageway, but not for the four bulkheads (walls) of either subcompartment. The actual material properties and thicknesses of the overheads and decks were used as model input for the validation, i.e., 0.95 cm thick steel. The thicknesses of the bulkheads were approximated as surface-area weighted averages. The estimated thicknesses for the steel bulkheads in the Fire Compartment and passageway were 0.76 cm and 0.80 cm, respectively.

As previously noted, there was only one gas sample point within the Fire Compartment. The gas was continuously suctioned from this point and traveled through tubing to the front of the ship where the oxygen, carbon dioxide, and carbon monoxide analyzers were located. There was a delay in the analyzer response time due to this travel time. The actual delay time is unknown. It was estimated, however, by determining the difference between the initial analyzer response to the fire and that of the nearest thermocouple. The analyzer data were then normalized using preignition ambient concentrations and the carbon monoxide to carbon dioxide mass ratio was calculated. A polynomial curve, fitted to the experimental data, was used to generate the model input for CO (the ratio of the mass of carbon monoxide to carbon dioxide produced by the oxidation of the fuel).

A nominal value of 0.06 was used for the OD parameter [8]. The OD parameter is the ratio of the mass of carbon to carbon dioxide produced by the oxidation of the fuel.

RESULTS

The experiment to be modeled began with ignition of a diesel pan fire at time zero. The combustion products from the fire rose to the top of the fire compartment until the depth of the upper layer was sufficient for the hot gases to flow under the soffit of the Fire Compartment door into the Passageway. The ceiling jet, consisting of these hot gases, traveled down the Passageway toward the thermocouple string at Location A. Some of the ceiling jet veered around the corner, heading toward the thermocouple next to the bi-flow probe in the overhead hatch at Location B. There are five events from the above scenario highlighted in Figure 11. These are: (1) time of pan fire ignition, (2) time at which combustion products flowed into the Passageway through the Fire Compartment door, (3) time at which ceiling jet reached Location A, (4) time at which ceiling jet reached Location B, and (5) time at which ceiling jet reached the end of the Passageway. Experimental times for Events 1, 3, and 4 can be obtained from thermocouple readings. These occurrences were at 0, 27, and 32 s, respectively.

CFAST Version 4.0.1 was used to generate model predictions for this validation. The Corridor Flow Submodel is an option that can be invoked by using the HALL keyword in the input file, along with the appropriate compartment as the corresponding parameter [3]. In the following discussion, the original model will refer to CFAST 4.0.1 without the Corridor Flow Submodel invoked, and the enhanced model will refer to CFAST 4.0.1 with the Corridor Flow Submodel invoked. The simulation

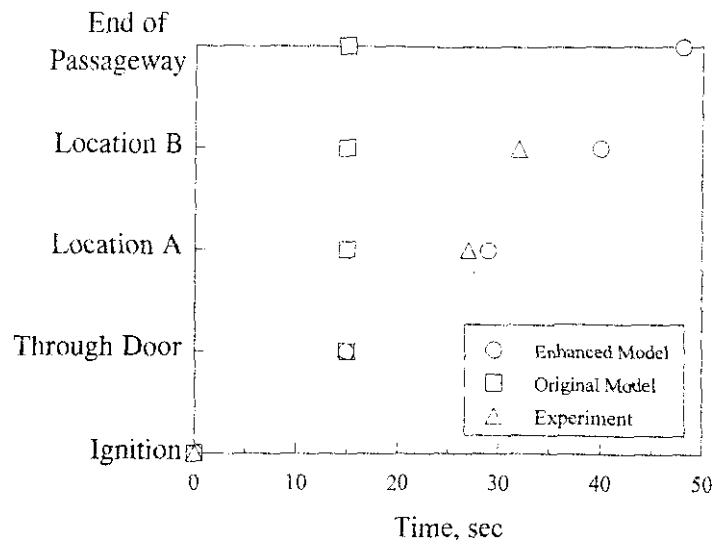


Figure 11. Comparison between model-predicted and experimentally determined ceiling jet progression.

with the original model was done using the actual Passageway dimensions (Sections 1-4). The enhanced model simulation utilized the modified dimensions as previously discussed (Sections 2 and 4) up until the time the ceiling jet reached the end of the Passageway. The actual Passageway dimensions were used for the remainder of the simulation. The model-predicted times for the five events described above are shown in Figure 11. Time zero was once again the time of pan fire ignition. Both the original model and the enhanced model predicted that the hot gases from the Fire Compartment would enter the Passageway at 15s. This is to be expected since the differences between the models occur after this point. The original model predicted that, 15s from ignition time, the hot gases would also reach both Locations A and B, as well as the end of the passageway. As previously described, the original model assumes a hot gas layer forms the instant that the hot gases pass under the Fire Compartment door soffit. The enhanced model predicted that Events 3 and 4 occurred at 29 and 40s, respectively. The enhanced model provides a more realistic prediction of the delay that occurs as the ceiling jet travels down the Passageway.

In addition to predicting the time at which the ceiling jet reaches specific locations within a corridor, the Corridor Flow Submodel predicts the temperatures at these locations. The temperature predictions are obtained by using the DETECT keyword in the input file to place detectors at specific locations. The temperature of the atmosphere at the location of the detector

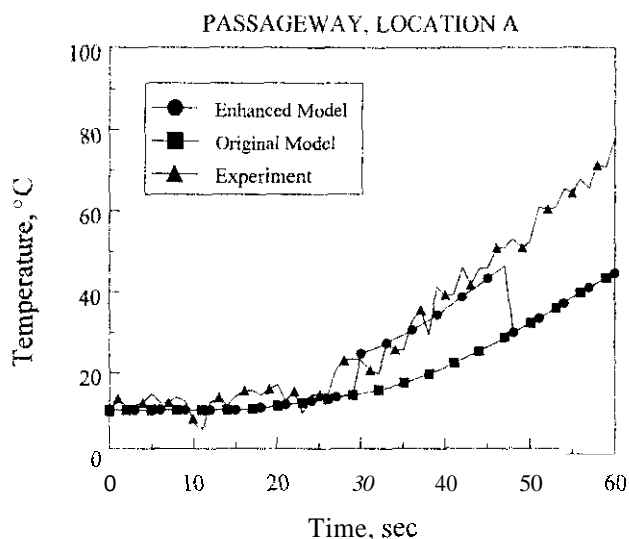


Figure 12. Comparison between model-predicted and experimentally determined temperature at Location A.

is reported in the output from CFAST. Figure 12 shows the temperature recorded by the top thermocouple in the string at Location A. The readings are normalized to 11°C (the ambient temperature), using thermocouple data recorded prior to ignition. This figure also shows the temperatures that both the original and enhanced model predicted would occur at this location. The curve predicted using the original model shows a gradual, smooth temperature increase with time. This is the average temperature of the upper gas layer. The curve predicted by the enhanced model is very close to this original curve until the ceiling jet reaches Location A. There is a sharp increase in temperature as the ceiling jet hits the location where the detector was placed. The predicted temperature agrees remarkably well with the experimentally determined temperature until the ceiling jet reaches the end of the corridor. 48 s from ignition. For times after 48 s, the model predictions, generated using the actual Passageway dimensions from time zero, are used.

Figure 13 shows the same information for Location B. The experimental data are from the thermocouple located in the overhead hatch. Again, these readings were normalized to 11°C using temperature data recorded prior to ignition. The temperatures predicted by the original model in Figures 12 and 13 are exactly the same. Recall that the original model, with its two layer assumption, predicts that temperatures at all upper layer locations along the Passageway are the same at any given time. The enhanced model

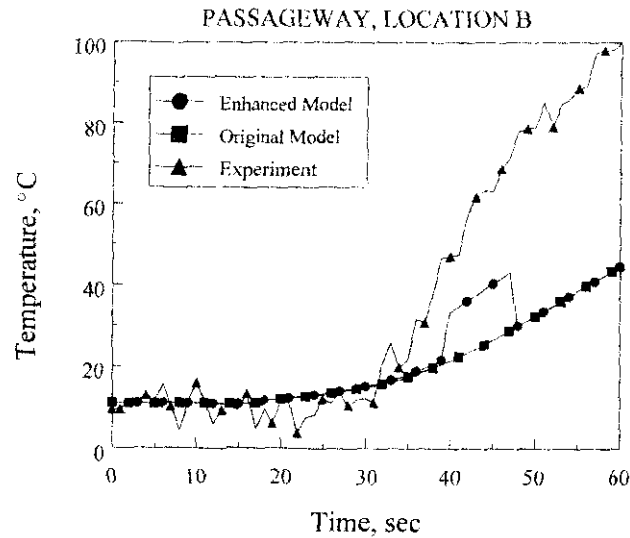


Figure 13. Comparison between model-predicted and experimentally determined temperature at Location B.

shows an increase 40s after ignition. The curve generated by the enhanced model does not follow the experimental data as well as it did at Location A. It is, however, much closer than the curve generated by the original model. Once the ceiling jet reaches the end of the Passageway, at 48s, the temperature predictions from the enhanced model fall back down to coincide with those from the original model.

MODEL SENSITIVITY TO INPUT ESTIMATES

The predictions of the Corridor Flow Submodel depend on the width of the corridor, or the Passageway in this case. Since the Passageway actually varied in width along its length, averages were used as model input for the predictions discussed above. To determine the sensitivity of the model to this particular input parameter, the enhanced model was rerun using the smallest (2.11 m) and the largest widths (2.39 m). The model-predicted times for Events 3 and 4 were within tenths of a second of the original predictions. Temperature predictions remained the same. The enhanced model was also rerun with the narrowest (0.318 cm) and widest (1.91 cm) bulkhead thickness. These changes had no effect on the model predictions.

CONCLUSIONS

Correlations were derived by performing numerical experiments using the computational field model, LES3D, to estimate ceiling jet arrival times and temperature fail-off rates for cases with various specified inlet ceiling jet temperatures and depth. These correlations were then used to develop a Corridor Flow Submodel which was recently added to the Consolidated Fire and Smoke Transport (CFAST) zone fire model, developed by NIST. Prior to the addition of the new submodel, CFAST did not properly account for the time it took a ceiling jet, entering at one end of a corridor, to travel down to the other end. Previously, CFAST assumed an upper layer, covering the entire ceiling area, would form instantaneously when the hot gases entered the corridor. All locations within this upper layer, and consequently, along the entire length of the corridor, would be at the same temperature. The new submodel enables CFAST to predict the flow of the ceiling jet down the corridor with time. CFAST also calculates, at any given time, the temperature distribution of the gases inside the ceiling jet.

The enhanced version of CFAST was used to model a real-scale experiment from the 688/SHADWELL test series. The Laundry Room in the 688/SHADWELL test series was partitioned into two subcompartments. One contained a pan fire and the other formed a corridor. Hot combustion products from the fire room entered the corridor and flowed along its length. Thermocouple readings were used to detect the movement and temperature of the ceiling jet along the corridor. CFAST, Version 4.0.1, provides the Corridor Flow Submodel as an option. When this option is invoked, CFAST predicts more realistic temperature distributions in the Laundry Room corridor. Both the time delay as the ceiling jet traveled down the corridor and the temperature predictions at two distinct corridor locations were comparable to those observed experimentally.

Even though the use of LES3D served as a good tool to design a corridor flow sub-model, further comparisons still need to be made between real-scale experiments and the zone fire model predictions. Such comparisons will allow for assessing the validity of the modeling assumptions, determining the accuracy of the predictions, and gaining better confidence in the use of this model.

ACKNOWLEDGMENTS

The work described in this report was funded by the Office of Naval Research, Code 334, under the Damage Control Task of the Surface Ship Hull, Mechanical and Electrical Technology Program (PE 0602121N).

REFERENCES

1. Peacock, R.D., Forney, G.P., Reneke, P., Portier, R. and Jones, W.W. "CFAST: The Consolidated Model of Fire Growth and Smoke Transport." National Institute of Standards and Technology, NIST TN 1299, 1993.
2. McGrattan, K., Rehm, R. and Baum, H. "Fire-Driven Flows in Enclosures." *J. Comp. Phys.*, Vol. 110, No. 2, 1994, pp. 285-291.
3. Forney, G.P. "A Note on Improving Corridor Flow Predictions in a Zone Fire Model." National Institute of Standards and Technology, NISTIR 6046, 1997.
4. Evans, D.D. "Ceiling Jet Flows", in Phillip J. DiNenno et al., editors. *SFPE Handbook of Fire Protection Engineering*, Chapter 1-9, McGraw-Hill Book Company, New York, first edition, 1989.
5. Cooper, L.Y. "Fire-Plume-Generated Ceiling Jet Characteristics and Convective Heat Transfer to Ceiling and Wall Surfaces in a Two-Layer Zone-Type Fire Environment: Uniform Temperature and Walls." National Institute of Standards and Technology, NISTIR 4705, 1991.
6. Cummings, W.M., Scheffey, J.L., Williams, F.W. and Tatem, P.A. "Test Plan, Submarine Ventilation Doctrine - Phase 1 (Fire Physics and Preliminary Ventilation System Testing), Revision 1." NRL Ltr Rpt 6180/0134, 20 June 1995.
7. Williams, F.W., Toomey, T.A. and Carhart, H.W. "The ex-SHADWELL Full Scale Fire Research and Test Ship," NRL Memorandum Report 6074, reissued Sept. 1992.
8. Hoover, J.B. and Tatem, P.A. "Application of CFAST to Shipboard Fire Modeling I. Development of the Fire Specification," NRL Memorandum Report 8466, 26 June 2000.